*Journal of the European Ceramic Society* **13** (1994) 25–31

# Gel Densification and Ceramic Sintering of $ZrO_2$–$Al_2O_3$ Composites

Wenbang Zhang & F. P. Glasser

Department of Chemistry, University of Aberdeen, Aberdeen AB9 2UE, UK

(Received 10 March 1993; revised version received 26 July 1993; accepted 10 September 1993)

***Abstract***

*The densification of $Al_2O_3$–$ZrO_2$ gels has been studied as a function of heating rate. The physical density of samples undergoing sintering was determined and their porosity measured by mercury intrusion. The shrinkage and flexural strengths of the ceramics were determined. Flexural strengths of 550–600 MPa could be achieved with pressureless sintering in the range 1575–1650°C.*

*Die Verdichtung von $Al_2O_3$–$ZrO_2$-Gelen wurde als Funktion der Heizrate untersucht. Die physikalische Dichte der gesinterten Proben wurde bestimmt und ihre Porosität mit Hilfe der Quecksilberintrusion gemessen. Die Volumenabnahme und die Durchbiegefestigkeit der Keramiken wurden bestimmt. Nach drucklosem Sintern bei 1575–1650°C konnten Durchbiegefestigkeiten von 550–600 MPa erzielt werden.*

*On a étudié la densification de gels d'$Al_2O_3$–$ZrO_2$ en fonction de la vitesse de chauffage. On a pu déterminer la densité en cours de frittage; la porosité a été mesurée par infiltration de mercure. Le retrait et la résistance à la flexion de ces céramiques ont été déterminés. Des résistances à la flexion de 550–600 MPa ont été obtenues par frittage naturel entre 1575 et 1650°C.*

## 1 Introduction

$Al_2O_3$–$ZrO_2$ composites remain an interesting subject for materials researchers because of their industrial and scientific uses.[1–4] Sol–gel processing arose as a new technology for the fabrication of high quality composite ceramics and glasses; for complex oxides, it achieves ultrahomogeneous mixing of the several components on a molecular scale. Liquid precursor technology offers processing advantages and gives flexibility in tailoring the composite chemistry to obtain the desired properties.

A new preparative method for $Al_2O_3$–$ZrO_2$ sol–gels from inorganic precursors has been developed and described previously.[5] The mechanism of the sol–gel transformation, the gel structure and its thermal decomposition have also been investigated.[6,7] The authors now report on the densification of the gels during sintering and their physical properties after firing.

Brinker & Scherer proposed that low-temperature densification is contributed to by at least four mechanisms:[8] (i) polymerization–condensation; (ii) capillary contraction; (iii) structural relaxation, and (iv) viscous sintering. Skeletal densification can be achieved by both polymerization reactions and relaxation,[9] i.e. the approach of the structure toward the configuration characteristic of the metastable liquid. It is expected that skeletal densification will make the greatest contribution to shrinkage for weakly crosslinked polymers; the $Zr^{4+}$ and $Al^{3+}$ gel polymers in this system are of this type.[6] The shrinkage will depend strongly on concentration, thermal history and temperature.

Sintering is the final stage in the transformation of a gel to a ceramic monolith. The removal of residual impurities, such as water and anions other than oxygen occurs with polycondensation and gradual disappearance of pores in the gel accompanied by densification and leads, under optimum conditions, to full densification.

The sintering rate of a gel is typically orders of magnitude faster than amongst bodies comprised of conventionally crushed crystalline powders because: (i) the gel contains smaller particles or pores with diameters typically in the order of 2–9 mm,[10] and (ii) gel densification during sintering is mainly achieved by viscous flow rather than by diffusion, as occurs in crystalline materials.[11] The main driving force



*Journal of the European Ceramic Society* 0955-2219/94/$7.00 

during gel sintering is the decrease of the large surface energy of the porous gel: at relatively low temperatures, sintering may be achieved and appreciable shrinkage can be observed even at extremely high viscosities.[10] The hydroxyl content of the gel markedly affects the viscosity: in general the higher the content of $OH^-$, the lower will be the viscosity of a gel.

However, during isothermal treatment at successively higher temperatures, water is lost progressively; the resulting condensation reactions will increase the crosslink density. Meanwhile, structural relaxation increases the skeletal density; these factors all lead to viscosity increases.[12] Thus, during an isothermal hold, the viscosity of a gel can rise by orders of magnitude, causing the sintering to halt, so that full densification is not easy to reach at lower hold temperatures. Therefore, it is advantageous to increase the temperature to compensate for structural relaxation and loss of $OH^-$. This suggests that the faster the heating rate, the lower will be the temperature at which densification is completed.[10] Nevertheless, the escape of volatiles cannot be too rapid as this will cause cracking. Pore closure may trap gases, which may later expand to cause serious bloating. If these problems can be avoided, densification may be achieved before or concurrently with crystallization.[13] So, the optimum heating schedule tends to be a compromise. Based on these findings, two groups of samples were prepared with different heating schedules.

## 2 Experimental

### 2.1 Sample preparation

Two series of $Al_2O_3$–$ZrO_2$ sol–gels were prepared:

Series A: 85·36% $ZrO_2$ + 10·44% $Al_2O_3$ + 4·2% $Y_2O_3$ (wt)

Series B: 17·28% $ZrO_2$ + 82·0% $Al_2O_3$ + 0·72% $Y_2O_3$ (wt)

The main zirconia precursor was a sol, which, upon analysis, corresponded to $Zr(OH)_{2\cdot95}(NO_3)_{1\cdot05}$ (3·65 M in Zr).[14] The alumina sol was $Al_2(OH)_5Cl$ (6·17 M in Al, from Albright & Wilson Ltd, West Midlands, UK). The $Y^{3+}$ solution, intended as a crystallochemical stabilizer for $ZrO_2$, was $Y(NO_3)_3$ (1·034 M in $Y^{3+}$). The mixed sol, with sufficient $Y^{3+}$ to achieve the target stabiliser ratio, was allowed to undergo gelation. The gels were aged at room temperature for one day, then pre-heated at 500°C, 700°C, 900°C for 3 h, to yield different powders, designated A500, A700, A900 and B500, B700, B900, respectively. Subsequently, all powders were ground in a zirconia automortar to reduce aggregation arising during the pretreatments. Except for A900, the powders were non-crystalline.

The powders were pressed under 295 MPa pressure at room temperature, with 1 min hold, to form pellets 13 mm diameter with thicknesses between 3·5 and 4·0 mm. The pellets were dried at 110°C for one day and fired as follows: from 100 to 500°C with a heating rate of 120°C/h with 2 h hold, then to a selected temperature (1425°C, 1500°C, 1575°C or 1650°C) at a heating rate of 240°C/h with a 3 h isothermal dwell time.

The gel composition selected for density and porosity measurements had 84·1% $ZrO_2$ + 15·9% $Al_2O_3$ (wt). It was aged for one day at room temperature, then heated from 100°C to high temperature with two heating programmes: (i) continuously heated from low temperature to high temperature in several steps with a 2 h hold at each intermediate temperature (referred to as 'slow heating'); (ii) heated from 100°C to 450°C at a heating rate of 450°C/h with a 2 h hold, then heated to the selected temperature at a rate of 1000°C/h with a 3 h hold (referred to as 'rapid heating').

### 2.2 Measurements

The density was measured by using a density bottle with toluene as a displacement liquid. The theoretical density, $D$, of a multicomponent system was calculated according to the following equation:

$$D = (W_1 + W_2 + \cdots + W_n)/(V_1 + V_2 + \cdots + V_n)$$

where $W_1$ and $V_1$, $W_2$ and $V_2$, to $W_n$ and $V_n$ are the weight and volume fraction of the first, the second to the $n$th component in the multicomponent system, respectively. A simple equation can be deduced from above equation:

$$D = 1/(m_1/D_1 + m_2/D_2 + \cdots + m_n/D_n)$$

where $m_1$ and $D_1$, $m_2$ and $D_2$, to $m_n$ and $D_n$ are the weight fraction and theoretical density of the first, the second, to the $n$th component, respectively. The theoretical densities of alpha-$Al_2O_3$ and tetragonal $ZrO_2$ are taken as 3·987 and 5·945 g/cm$^3$, respectively.

Flexural strengths were obtained in three-point loading. The calculation of flexural strength $S_f$ is as follows:[3]

$$S_f = 3PL/(2bh^2)$$

where $P$ is maximum load, $L$ is span length of loading at two sides (which is 9 mm), $h$ and $b$ are height and width of cracking surface, respectively. This equation is valid only if a linear elastic stress distribution is assumed in the bending member.

A Micromeritics 9300 porosimeter was used to determine porosity changes; it is capable of exerting a maximum pressure of 207 MPa (30 000 psi). The

specimens were immersed in mercury in a sealed system; by applying a pressure to the mercury it ingressed the pores in the specimens at a rate dependent on the pore size and pressure of mercury: the mercury contact angle is taken as 140°.

## 3 Results and Discussion

### 3.1 Densification of gel during sintering

$ZrO_2$–$Al_2O_3$ gel forms by the hydrolysis and polymerization of $Zr^{4+}$ and $Al^{3+}$ at low pH by acid catalysis.[5,6] This leads to formation of gels having a finer, denser structure. This structure is not particulate, but consists of comparatively linear, lightly crosslinked polymeric clusters.[11] When these gels are heated, hydroxyl groups are removed by condensation reactions, leading to a large weight loss.[5,7] These reactions produce new crosslinks and stiffen the structure.

Figures 1 and 2 show how $Al_2O_3$–$ZrO_2$ gel density, micropore volumes and specific surface areas change at different temperatures during

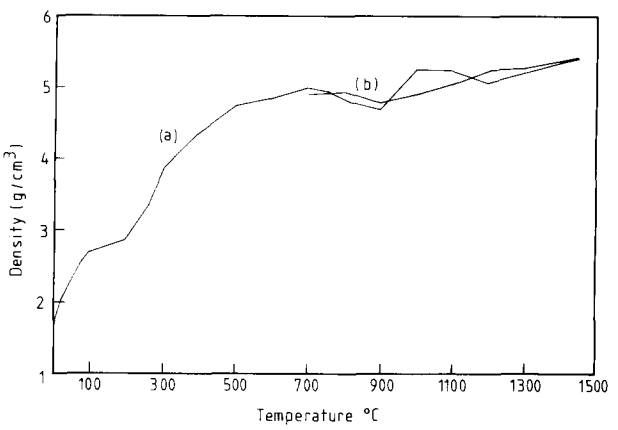


**Fig. 1.** Gel density at different temperatures, see text for details. (a) Slow heating; (b) rapid heating. Relative accuracy of determinations, which are themselves the average of three determinations, is ±0·048 density units.

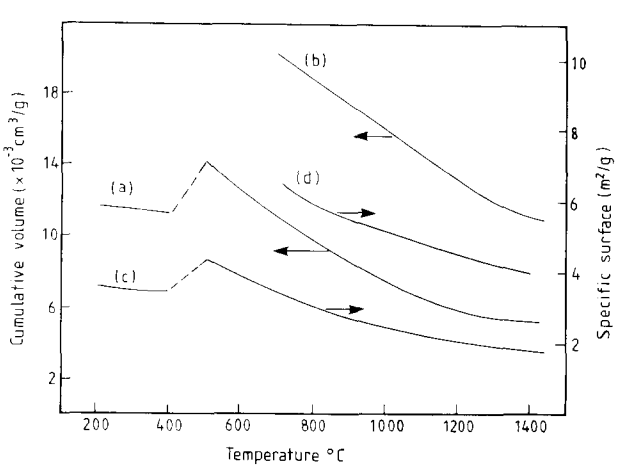


**Fig. 2.** Pore volumes ($d < 50$ nm) and specific surface at different temperatures: (a) pore volume–slow heating; (b) pore volume–rapid heating; (c) specific surface–slow heating; (d) specific surface–rapid heating.

sintering. Results are discussed first for the 'slow-heated' samples.

At 100°C, the gel lost about 50% of its initial weight.[5] The pores contract rapidly because of strong capillary forces. The density increases from 1·56 g/cm$^3$ at room temperature to 2·71 g/cm$^3$ at 100°C; see Fig. 1(a). At 200°C, the gel lost a further 6% weight, but did not change its structure significantly. The density increases from 2·71 g/cm$^3$ at 100°C to 2·86 g/cm$^3$ at 200°C. When rewetted after drying at 200°C, the heated gel will still redisperse and gelatinize, although instead of giving a clear solution, it gives a milky dispersion because of the heterogeneous nature of the resulting dispersion.

At 300°C, the gel structure was destabilized: most of its $NO_3^-$ and $H_2O$ were lost and it would no longer gelatinize when redispersed in water. Large increases in density occur: from 2·86 g/cm$^3$ at 200°C to 3·82 g/cm$^3$ at 300°C. These arise from rearrangements in the gel structure. Hydroxyl groups and anions are removed by condensation reactions, leading to a large weight loss. These reactions produce more new crosslinks and stiffen the gel structure, with the result that the gel becomes physically much harder after heating at 300°C.

At 400°C, the gel loses almost all its remaining $OH^-$ and anions; further structural rearrangement takes place, allowing the solid phase to densify and increase in viscosity. Mercury porosimetry shows that the volume of large pores, above 0·15 μm, is always very small. Therefore changes in the volume of large pores during heating are not significant. Below 0·15 μm, the accessible pore volume does not change very much; the bulk density continues to increase.

During desiccation the polymer clusters in the gel are compacted and further crosslinked until the gel network can resist the compressive action of surface tension, at which point further densification leads to the creation of porosity.[13] However, the specific surface area and cumulative porosity with diameters < 50 nm in the low temperature (< 400°C) product, shown in Fig. 2(a) and (c) is quite low. One possible explanation is that the gel structure is not stiff; it collapses during intrusion when high pressures are applied. Another possibility is that, owing to the difficulty of drying, some liquid is still present in pores, thereby blocking access by mercury. A third possibility is that much of the residual porosity is isolated; the volume of this hypothetical porosity is, however, temperature-dependent. It is also noteworthy that the intrinsic gel pores range in size between 2 and 9 nm,[10] and mercury intrusion, which can only detect pores greater than 7 nm, may not access much of the gel porosity. Thus, during sintering, the amount of porosity could be quite

significantly greater than the accessible porosity. This is particularly so during the early stages of heating, before crystallization occurs. Prior to crystallization, it is difficult to compare density and porosity functions, because the mass is changing continuously and the true density of particles—decomposed gels—cannot be measured or predicted. However, once crystallization has finished, or nearly so, the situation is more amenable to analysis.

The XRD, IR and density results disclose that densification continues,[7] but that no significant structural changes occur up to 800°C. Figure 2(a) and (c) show that specific surface and cumulative porosity with diameters $<50$ nm decreases gradually. However, the density decreases somewhat in this range; from 4·82 g/cm$^3$ at 800°C to 4·70 g/cm$^3$ at 900°C. XRD results show that the gel begins to crystallize at 800°C.[7] At 900°C, as crystallization proceeds, the crystallites grow markedly in size, which may be the cause of the lowered density, although the mechanism is unclear.

During continuous heating to higher temperature, gel densification continues as shown in Fig. 1(a): surface and porosity with diameters $<50$ nm decrease. It is possible that another region of density decrease occurs in the range 1100–1200°C; from 5·22 g/cm$^3$ at 1100°C to 5·05 g/cm$^3$ at 1200°C. The principal change in structure between these temperatures is the transformation of $ZrO_2$(t) to $ZrO_2$(m).

From 1200°C to 1450°C, the volume of large pores remains essentially unchanged, while both the volume of smaller pores and specific surface continue to decrease gradually while the density increases.

The gel is virtually free of large pores, $>0{\cdot}15\ \mu$m. This situation continues during heating: the gel shrinks and densifies without formation of large pores. The cumulative porosity graph, Fig. 2, shows an apparent reduction in accessible porosity with continued heating, but does not give a complete picture of the pore size distribution. It is, however, sufficient to show that the gels can undergo sintering and densification without development of coarse pores and, as they evolve ceramic structure, the accessible porosity shifts towards a finer pore regime.

It is better if densification can be completed before crystallization occurs, because the densification rate controlled by viscous flow in the gel sintering is orders of magnitude faster than by diffusion during conventional sintering of crystalline materials.[10,15] Therefore, the most favourable course for densification of a monolithic gel is to sinter to close to full densification but retain some ability to accommodate further shrinkage arising from progressive crystallization. All samples in these experiments were heated from 100°C to high temperature in several steps with 2 hour hold at each intermediate temperature, so the bulk of the crystallization occurred after the gel had become rather rigid. The most important factors that can be used to control the degree of crystallization are composition, microstructure, applied pressure during sintering, physical inhomogenities, such as clusters or chemical dopants and the extent to which heterogeneous nucleation occurs. Reducing the pore size or applying pressure during sintering speeds sintering without significantly affecting crystal nucleation or growth.[16,17] Hot pressing during sintering is often used, but is not necessarily the most desirable solution to achieve good densification: indeed, densities of 4·87–4·97 g/cm$^3$ were obtained before crystallization occurs from essentially non-crystalline dehydroxylated gels simply by optimizing the heating programme by correlating data obtained on porosity and phase development with density.

Figure 1(b) shows density changes of 'rapidly-heated' samples above 700°C. A density decrease occurs at 900°C, but without a decrease at 1200°C. It is possible that sintering with rapid heating rate at high temperature compensates for the adverse affect of the phase transformation in zirconia on density. The density increases gradually from 900°C to 1450°C. It achieves near-theoretical density at 1450°C (5·42 g/cm$^3$), supporting the view that it is generally preferable to sinter gels at rapid heating rates to achieve densification which will shorten sintering time and enable full densification to be achieved at relatively low temperatures.

However, excessively rapid heating will also cause trapping of evolved gases that can crack or bloat the gel. Figure 2(b) and (d) show that rapid heating results in both an increase in pore volume with diameter $7 \rightarrow 50$ nm and specific surface (for pores with diameters greater than 7 nm). Therefore, it is suggested that the heating rate in this research may not be the best compromise and may be slightly too rapid. However, the specimens used were physically small; for large specimens, the physics of heat transfer and consequences of differential temperatures will also need to be addressed, so the schedules used may indicate what can be typically achieved with larger specimens.

### 3.2 Physical properties changes of $Al_2O_3$–$ZrO_2$ composites during sintering

The physical properties such as density, shrinkage and flexural strength of final fired $Al_2O_3$–$ZrO_2$ composites derived from sol–gel processing depend strongly on composition, preparation and heating programme. Figure 3 shows that shrinkage occurs from 1400°C to 1575°C, but slows after 1575°C for A700 and A900 samples. However, the course of shrinkage for A500 is different: it is increased sharply

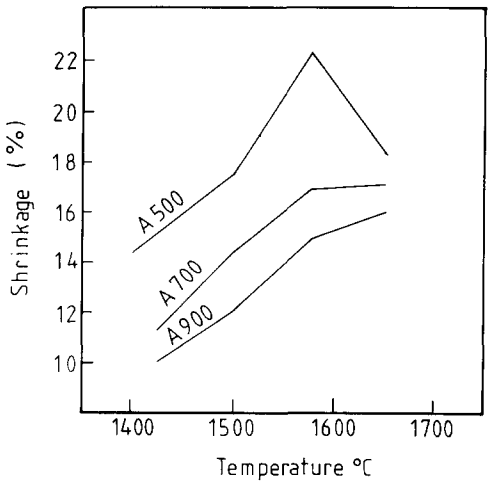


**Fig. 3.** Shrinkage versus temperature, $Al_2O_3$–$ZrO_2$ gel, series A. The error in shrinkage is estimated to be ±0·61%.

by firing at 1575°C but decreased after further firing at 1650°C. In addition, for the same firing temperature, shrinkage increases in the order: A500 > A700 > A900. Figure 4 gives apparent density changes of series A samples after firing at different temperatures, which shows much the same order as in Fig. 3. Data for the density–temperature curves of both A500 and A900 almost overlap at lower temperatures, but separate at 1575°C: A900 is still increasing in density while A500 is decreasing.

Since gel densification begins from the smallest particles, attempts were made to examine particle size by TEM:[18] they increase in the order A900 > A700 > A500. If small particles provide the large driving force for densification, the rate of densification predicted from this criteria will be A500 > A700 > A900. On the other hand, the densification rate is much faster when transport occurs by viscous flow than by diffusion. A900 contains crystalline material (with some amorphous phase), but A500 and A700 precursors are almost entirely amorphous.[7] Therefore, densification of A900 is the slowest of the series. It is suggested that densification of A500 is completed between 1575 and 1650°C, but that densification is destroyed at 1650°C because of over-firing, which may lead to coarsening of crystalline particles and a second recrystallization with discontinous or exaggerated grain growth.

Chemical decomposition of these gels is essentially completed at 400°C;[7] they begin to crystallize at 800°C and their density–temperature curve achieves the first concave portion at 900°C; see Fig. 1. The gel densifications after firing at 500°C and 900°C are very similar, so the curves, A500 and A900 almost overlap below 1575°C but diverge at and above 1575°C. The apparent density of A900 is still increasing at 1650°C, while that of A500 is decreasing. Therefore, A900 needs the highest temperature to achieve complete densification.

Series B samples behave differently; Fig. 5 shows the shrinkages for B500, B700 and B900, which have the same tendency: the shrinkages increase in the order B500 > B700 > B900. However, comparing apparent density–temperature curves, B900 is intermediate, between B500 and B700, as shown in Fig. 6. X-ray diffraction patterns show that all three (B500, B700, B900) are amorphous until they begin to crystallize at 1000°C.[18] Therefore, in the $Al_2O_3$–$ZrO_2$ gel system, the higher the content of $Al_2O_3$, the higher the temperature at which crystallization occurs. $Al_2O_3$ significantly retards the crystallization of $ZrO_2$,[18] probably by acting as a grain growth inhibitor for zirconia.[19] On the other hand, $Al_2O_3$ needs a higher temperature to crystallize than $ZrO_2$.[18] Therefore, the mechanism of densification for B500, B700 and B900 is primarily viscous flow; the main difference between B500, B700 and B900 is in particle size.

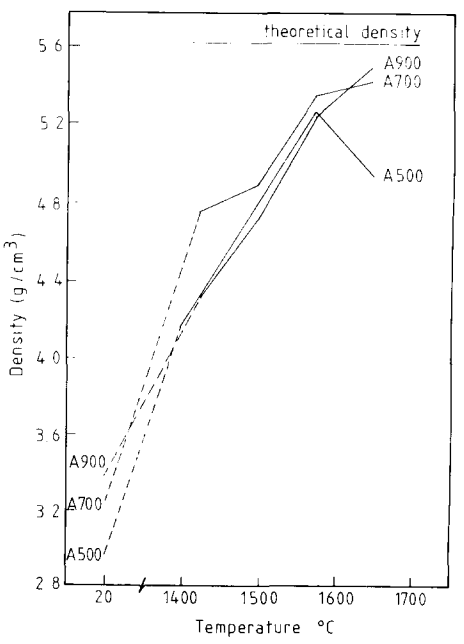


**Fig. 4.** Apparent density versus temperature, $Al_2O_3$–$ZrO_2$ gel, series A. The densities were measured by toluene displacement and are accurate to ±0·051 density unit.

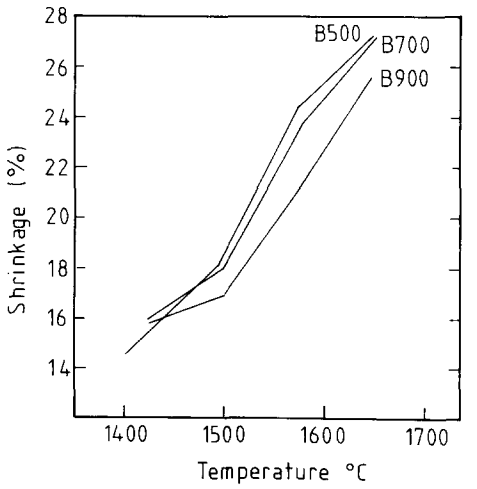


**Fig. 5.** Shrinkage versus temperature, $Al_2O_3$–$ZrO_2$ gel, series B. The error in shrinkage is estimated to be ±0·29%.

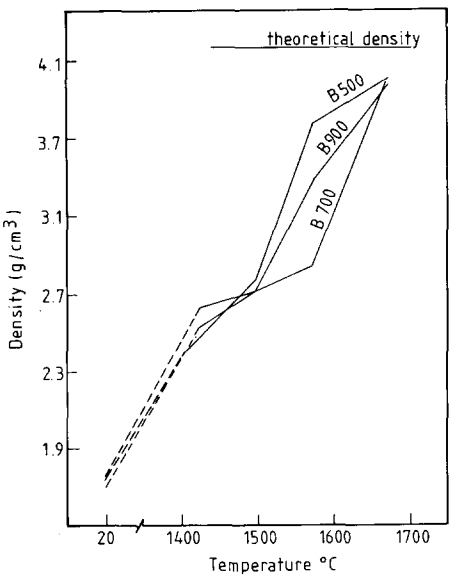


**Fig. 6.** Apparent density versus temperature, $Al_2O_3$–$ZrO_2$ gel, series B. The densities were measured by toluene displacement and are accurate to ±0·045 density unit.

The flexural strength is shown in Figs 7 and 8. For series A materials, the best pretreatment temperature is 700°C, in terms of achieving the highest flexural strengths. For A900, densification was slow and crystalline particles coarsened rapidly during sintering at high temperature. For A500, densification occurred rapidly because of its very high specific area, resulting from low pretreatment temperature. After sintering, A500 may still retain some pores, on account of its very low initial green density. Its flexural strength and final density, therefore, are relatively low. In series B, the development of flexural strength after sintering at different temperatures correlates well with shrinkage and apparent density changes, with B700 giving the best results.

The deviation of the flexural strength is given in Table 1. Ten specimens were used for each firing cycle. The highest and lowest values were discarded

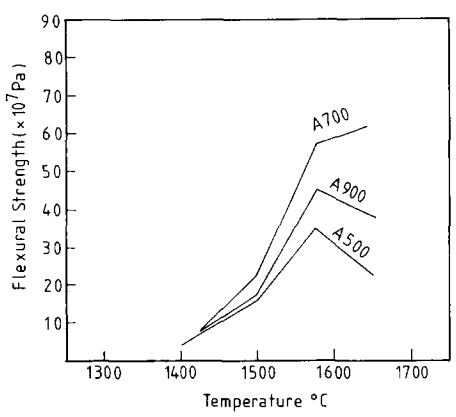


**Fig. 7.** Flexural strength of $Al_2O_3$–$ZrO_2$ ceramics derived from sol–gel, and fired at different temperatures (series A). Standard deviations are given in Table 1.

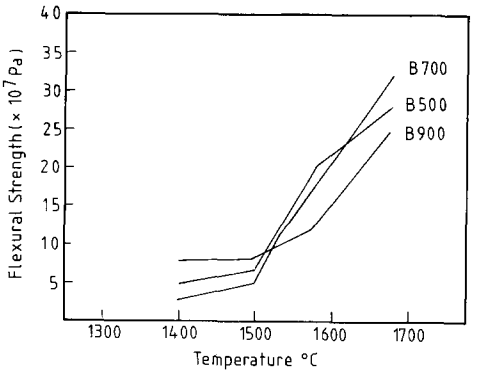


**Fig. 8.** Flexural strength of $Al_2O_3$–$ZrO_2$ ceramics derived from sol–gel, and fired at different temperatures (series B). Standard deviations are given in Table 1.

and the remaining eight values used. The deviation is

$$d = (|S_{f1} - S| + |S_{f2} - S| + \cdots + |S_{fn} - S|)/(nS)$$

where $S$, $n$, $S_{f1}$, $S_{f2}$ to $S_{fn}$ are the mean flexural strength, number of replicate specimens, the flexural strengths of the first specimen, the second specimen, etc. and the $n$th specimen, respectively. Except for A500 samples, the deviations are reasonable; most are below 0·10.

The flexural strengths of series A are generally much higher than that of series B, because series A contains much more stabilized tetragonal $ZrO_2$. Compared to series A, series B powder precursor needs higher temperatures or longer sintering times to achieve satisfactory densification and good flexural strengths.

The flexural strength results are probably not optimal, because of the relatively low green densities. Figures 4 and 6 show that the green densities of all samples are too low; after final sintering at different temperatures, the apparent densities are still much less than theoretical densities. But the flexural strengths are still higher than that of normal $ZrO_2$–$Al_2O_3$ composites, which lie in the range 400–550 MPa[20] and are in flexural strength range of Y-PSZ ceramics, which are about 500–800 MPa.[1] Practical ceramics can thus be obtained using sol–gel processing, without the need to hot-press.

## 4 Conclusion

Gel densification is orders of magnitude faster than densification of conventionally crushed and mixed

**Table 1.** Standard deviation of flexural strengths

| *Firing temperature* (°C) | *Samples* | | | | | |
|---|---|---|---|---|---|---|
| | *A500* | *A700* | *A900* | *B500* | *B700* | *B900* |
| 1 500 | 0·343 | 0·099 | 0·118 | 0·099 | 0·043 | 0·109 |
| 1 575 | 0·168 | 0·074 | 0·060 | 0·082 | 0·047 | 0·098 |
| 1 650 | 0·196 | 0·050 | 0·325 | 0·080 | 0·043 | 0·112 |

crystalline powders because of viscous flow sintering mechanism and its high specific surface area. The density increases gradually during heating from low to high temperature, but there are two concave portions at 900°C and 1200°C, respectively. Crystallization and phase transformation are probably responsible for the first and second decreases, respectively.

The shrinkage, apparent density and flexural strength of $ZrO_2$–$Al_2O_3$ gels during sintering is dependent strongly on the pretreatment temperature and firing temperature. The higher the pretreatment temperature, the lower will be the shrinkage. After complete decomposition, the higher the pretreatment temperature, the higher becomes the temperature necessary to achieve complete densification. If pretreatment causes crystallization, the subsequent densification is much slower and much higher temperatures are required to achieve complete densification. Good flexural strengths in $ZrO_2$–$Al_2O_3$ composites, using sol–gel processing, can be achieved by appropriate pretreatment and sintering programmes.

## Acknowledgements

The authors thank Banbury Laboratory, Alcan International Limited, Oxon, UK, for financial support.

## References

1. Cannon, W. R., Transformation toughened ceramics for structural application. In *Structural Ceramics*, ed. J. B. Wachtman, Jr, *Treatise on Materials Science and Technology*, Vol. 29. Academic Press, Inc., San Diego, CA, 1989, pp. 195–228.
2. Faber, K. T., Toughening in $ZrO_2$-based materials. In *Advanced Ceramics*, ed. S. Saito. Oxford University Press, Oxford, UK, 1988, pp. 76–94.
3. Claussen, N., Fracture toughening of alumina with an unstabilized $ZrO_2$ dispersed phase. *J. Am. Ceram. Soc.*, **59** (1976) 49–51.
4. Lange, F. F., Transformation toughening. Part 1: size effects associated with the thermodynamics of constrained transformations. *J. Mater. Sci.*, **17** (1982) 225–34.
5. Zhang, Wenbang & Glasser, F. P., The preparation of $Al_2O_3$–$ZrO_2$ sol gels from inorganic precursors. *J. Eur. Ceram. Soc.*, **11** (1993) 143–7.
6. Zhang, Wenbang & Glasser, F. P., Condensation and gelation of $ZrO_2$–$Al_2O_3$ sols. *J. Mater. Sci.*, **28** (1993) 1129–35.
7. Zhang, Wenbang & Glasser, F. P., The structure and decomposition of $Al_2O_3$–$ZrO_2$ gels. *J. Eur. Ceram. Soc.*, **11** (1993) 149–55.
8. Brinker, C. J. & Scherer, G. W., Sol → gel → glass: I. Gelation and gel structure. *J. Non-Cryst. Solids*, **70** (1985) 301–22.
9. Brinker, C. J., Scherer, G. W. & Roth, E. P., Sol → gel → glass: II. Physical and structural evolution during constant heating rate experiments. *J. Non-Cryst. Solids*, **72** (1985) 345–68.
10. Scherer, G. W., Sintering of gel. In *Sol–Gel Science and Technology, Proceedings of the Winter School on Glasses and Ceramics from Gels*, ed. M. A. Aegerter, M. Jafelicci, Jr, D. F. Souza & E. D. Zanotto. Sao Carlos, SP, Brazil, August 1989, pp. 221–56.
11. Brinker, C. J. & Scherer, G. W., *Sol–Gel Science: The Physics and Chemistry of Sol–Gel Processing*. Academic Press, San Diego, CA, USA, 1990, pp. 675–744.
12. Gallo, T. A. & Klein, L. C., In *Better Ceramics Through Chemistry II, Mater. Res. Soc. Symp. Proc.*, Vol. 73, ed. C. J. Brinker, D. E. Clark & D. R. Ulrich. North-Holland, NY, 1986, pp. 245–50.
13. James, P. F., The gel to glass transition: chemical and microstructural evolution. *J. Non-Cryst. Solids*, **100** (1988) 93–114.
14. Woodhead, J. L., Sol–gel process to ceramic particles using inorganic precursors. *J. Mater. Ed.*, **6** (1984) 887–925.
15. Hopper, R. W. & Uhlmann, D. R., On diffusive creep and viscous flow. *Mater. Sci. Eng.*, **15** (1974) 137–44.
16. Zarzycki, J., In *Advances in Ceramics*, Vol. 4, American Ceramic Society, Columbus, OH, 1982, pp. 204–16.
17. Zarzycki, J., Gel → glass transformation. *J. Non-Cryst. Solids*, **48** (1982) 105–16.
18. Zhang, Wenbang, Lachowski, E. E. & Glasser, F. P., Structural evolution of $ZrO_2$–$Al_2O_3$ gel during sintering. *J. Mater. Sci.*
19. Murase, Y., Kato, E. & Daimon, K., Stability of $ZrO_2$ phase in ultrafine $ZrO_2$–$Al_2O_3$ mixtures. *J. Am. Ceram. Soc.*, **69** (1986) 83–7.
20. Sudo, H. & Sakuma, K., Recent study on $ZrO_2$ transformation toughening. *J. Japan. Metal. Soc.*, **22** (1983) 887–93.